PROCEEDINGS OF SCIENCE

Radiation Hard Pixel Sensors for the Phase 2 Upgrade of the CMS Inner Tracker

Georg Steinbrück[a,*] for the Tracker Group of the CMS Collaboration

[a] *Hamburg University, Institute for Experimental Physics,*
Luruper Chaussee 149, 22761 Hamburg, Germany

E-mail: georg.steinbrueck@uni-hamburg.de

The Inner Tracker (IT) of the Compact Muon Solenoid (CMS) experiment of the Large Hadron Collider at CERN will be upgraded for the High-Luminosity LHC (HL-LHC). The expected integrated luminosity at the end of the HL-LHC running phase is at least 3000 fb^{-1}, corresponding to a 1 MeV neutron equivalent fluence of $\Phi_{\text{eq}} = 2.6 \times 10^{16}\,\text{cm}^{-2}$ and a total ionizing dose (TID) of 13 MGy at the innermost layer of the IT. All the layers of the IT (except for the innermost barrel layer) will be equipped with planar n^{+}-p pixel sensors with an active thickness of 150 µm and pixel sizes of 25 µm × 100 µm. The innermost barrel layer will feature 3D silicon sensors owing to their excellent radiation hardness and lower power consumption; it is foreseen to be exchanged at least once during HL-LHC operation. Planar and 3D prototype sensors were bump bonded to the CMS prototype chip (CROCv1), implemented in 65 nm CMOS technology. In an extensive qualification campaign, sensor-chip assemblies were tested in the lab and at the CERN and DESY testbeam facilities before and after proton irradiation up to $\Phi_{\text{eq}} = 2 \times 10^{16}\,\text{cm}^{-2}$, exceeding the expected maximum fluences. In this paper, more recent measurements of the hit efficiency, spatial resolution, and noise studies are presented after proton irradiation at the CERN Proton Synchrotron (PS) up to $\Phi_{\text{eq}} = 1 \times 10^{16}\,\text{cm}^{-2}$. For all parameters investigated, the results meet or exceed the CMS specifications. Based on the results of these measurements and on tracking and thermal simulations, sensor designs were chosen for the IT Upgrade and CMS has started to prepare for the (pre)-production phase of pixel sensors and modules. The main lessons learned on the path to the choice of a radiation hard sensor are summarized.

6th International Conference on Technology and Instrumentation in Particle Physics (TIPP2023)
4 - 8 Sep 2023
Cape Town, Western Cape, South Africa

*Speaker

PoS(TIPP2023)065

1. Introduction

The Large Hadron Collider (LHC) at CERN will be upgraded in order to increase the instantaneous luminosity from the current $2 \times 10^{34}\,\mathrm{cm}^{-2}\,\mathrm{s}^{-1}$ to $7.5 \times 10^{34}\,\mathrm{cm}^{-2}\,\mathrm{s}^{-1}$, boosting the physics potential of the LHC experiments [1]. An integrated luminosity of 3000 to 4000 fb^{-1} will have been delivered by the end of the 10 year High-Luminosity LHC (HL-LHC) program, which is an increase by about a factor of ten with respect to the first three runs of the LHC ending in 2025 [2]. The increased instantaneous luminosity means a higher rate of proton-proton interactions, on the order of 200 per bunch crossing, and thus a higher particle fluence and total ionizing dose (TID) in the detectors. The Compact Muon Solenoid (CMS) detector [3, 4] will be upgraded in order to maintain or even improve its measurement capabilities under such challenging conditions.

This paper focuses on the upgrade of the CMS Inner Tracker (IT) [5], which is entirely composed of silicon pixel detectors. The upgraded IT will feature a two-phase CO_2 cooling system with a liquid CO_2 temperature of −33 °C, leading to sensor temperatures in the range of −20 to −15 °C. A layout of the CMS IT is shown in Fig. 1. The IT is constructed in three parts: the Tracker Barrel Pixel Detector (TBPX), the Tracker Forward Pixel Detector (TFPX), and the Tracker Endcap Pixel Detector (TEPX). In the innermost layer of TBPX, a non-ionizing energy loss (NIEL)

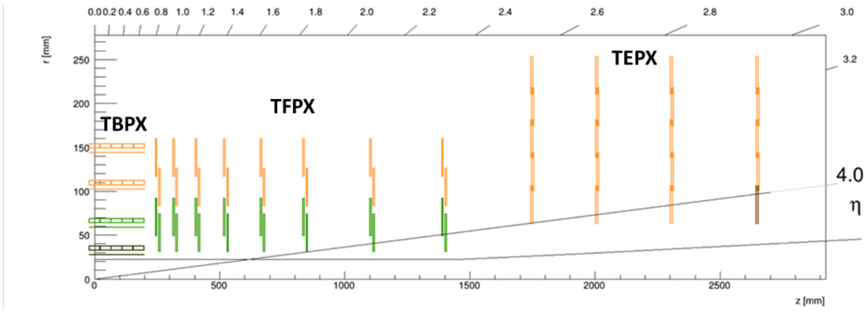

Figure 1: Layout of the CMS Inner Tracker (IT) for Phase-2. In the IT, pixel detector modules with 2×2 readout chips (shown in yellow) and 1×2 readout chips (shown in green) are used [5]. The innermost part of TBPX (shown in black) comprises 1×2 modules with two individual 3D sensors. The innermost ring of disc 4 of TEPX (shown in brown) consists of 2×2 modules and also provides data to the luminosity system. The lower black line represents the outer radius of the beam pipe.

corresponding to a 1 MeV neutron equivalent particle fluence of $\Phi_{eq} = 2.6 \times 10^{16}\,\mathrm{cm}^{-2}$ and a total ionizing dose (TID) of 13 MGy are expected after 3000 fb^{-1} of integrated luminosity. In the second layer, the fluence will be $\Phi_{eq} = 0.7 \times 10^{16}\,\mathrm{cm}^{-2}$ and the TID 4 MGy. In the first ring of the TFPX, a maximum fluence of $\Phi_{eq} = 1.7 \times 10^{16}\,\mathrm{cm}^{-2}$ and a TID of 11 MGy are expected. Owing to their radial orientation, the fluence in the forward sections will vary up to about a factor of two within one module. Neither the sensors nor the readout chips are not expected to be operable significantly above $\Phi_{eq} = 1 \times 10^{16}\,\mathrm{cm}^{-2}$ and 10 MGy, respectively. Therefore, a replacement of layer 1 of TBPX and ring 1 of TFPX are foreseen midway through the HL-LHC running period. All the layers of the IT (except for the innermost barrel layer) will be equipped with planar n^+-p pixel sensors with an active thickness of 150 µm and pixel sizes of 100 µm × 25 µm. The innermost barrel layer will feature 3D silicon sensors because of their excellent radiation hardness and lower power consumption [6]. The 3D sensors will have the same pixel dimensions and active thickness as the planar sensors. The long pixel side is oriented parallel to the beam axis (along z) in the barrel and radially outwards (along r) in the forward and endcap discs. The requirements for pixel sensors for the CMS IT can be found in Table 1. In this paper, results from laboratory and testbeam measurements with prototype sensor-readout chip assemblies are presented.

Table 1: Selected requirements for planar and 3D pixel sensors. The hit efficiency is denoted by ϵ_{hit}. (*) annealing at 60 °C for 1 hr.

Parameter	Planar	3D
active thickness, polarity	150 μm n^+p, pstop	150 μm n^+p, pspray
depletion voltage, V_{fd}	<100 V	<10 V
breakdown voltage before irradiation	>350 V	$>V_{fd}$ + 35 V
leakage current, 20 °C before irradiation	<0.75 μAcm^{-2} at V_{depl} + 50 V	<2.5 μAcm^{-2} at V_{depl} + 25 V
leakage current, -25 °C at $\Phi_{eq} = 5 \times 10^{15}$ cm^{-2}(*)	<45 μAcm^{-2} at 600 V	
leakage current, -25 °C at $\Phi_{eq} = 1.5 \times 10^{16}$ cm^{-2}		<100 μAcm^{-2} at V_{op}(<200 V)
ϵ_{hit} before irradiation	>99%	>96(97)% at 0°(10°) angle
ϵ_{hit} at $\Phi_{eq} = 5 \times 10^{15}$ cm^{-2}	>99%	
ϵ_{hit} at $\Phi_{eq} = 1 \times 10^{16}$ cm^{-2}	>98%	
ϵ_{hit} at $\Phi_{eq} = 1.5 \times 10^{16}$ cm^{-2}		>96(97)% at 0°(10°) angle

The CMS readout chip

The development of a readout chip for the Phase 2 ATLAS and CMS pixel detectors was done within the common framework of the RD53 Collaboration [7]. In this paper, the full-size prototype chip, RD53B-CMS or CROCv1 (CMS ReadOut Chip) [8, 9], is used, whereas the final production chip will be the CROCv2. The chip features the Linear analog front-end design. It consists of 336 rows and 432 columns, for a total of 145,152 pixels, with a bump bond pattern of 50 μm × 50 μm. Manufactured using 65 nm CMOS technology, the chip features a radiation-hard design and has been validated up to a TID of 10 MGy. The chip allows for serial powering, has an adjustable online threshold down to around 1000 electrons, and a Time-over-Threshold (ToT) charge measurement with a 4-bit resolution time-to-digital converter at 40 MHz.

Prototype pixel modules

A pixel module consists of a silicon pixel sensor bump bonded to one or more readout chips to form a hybrid pixel detector. In this study, only prototype single-chip modules are tested. The pixel cell for a planar sensor is shown in Fig. 2. To interconnect a sensor with 100 μm × 25 μm pixels to the CROC chip with a 50 μm × 50 μm cell size and bump bond pattern, a metal routing from the implants to the bump bond pads on the sensors is required. To maximize the hit efficiency, the planar sensors do not have a biasing scheme like a punch-through bias dot. This choice makes it

PoS(TIPP2023)065

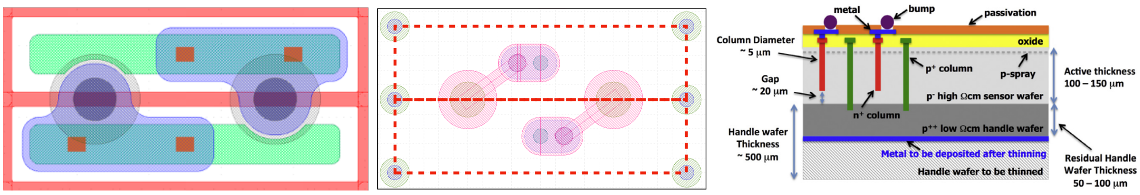

Figure 2: The layout for two adjacent 100 µm × 25 µm pixel cells in a planar CMS sensor. The color code indicates the various mask layers: n^+ implant (green), p-stop implant (red), metal contact via (orange), metallization (blue), and opening in the passivation for bump bonding (purple) (left). Two adjacent pixel cells of a 3D sensor , depicted by dashed red lines. The ohmic columns, depicted by blue circles, are located at the corners of the pixel cell. In the center of the pixel cell there is the n-column surrounded by a metal pad. The large green circles correspond to the ROC bump pads. The routing between the sensor and the readout chip is depicted in pink (center). Cross section of FBK 3D sensor (right) .

impossible to fully deplete the sensors on a wafer to identify faulty sensors by their current-voltage characteristics before the non-reversible bump bonding process. The prototype planar sensors discussed in this paper were produced by Hamamatsu Photonics K.K. [10], while the 3D sensors were produced by FBK [11]. The details of the planar sensor design, production and previous studies are described in Refs. [12–14]. The sensors were bump bonded to CROCv1 readout chips with SnAg bumps at the Fraunhofer Institute for Reliability and Microintegration (IZM) in Berlin, Germany [15].

2. Hit efficiency

A hit efficiency close to 100% is required for efficient particle tracking given the limited number of layers in the IT. To determine the efficiency, first, pixels are masked as noisy if they have an occupancy above 1×10^{-4}. The percentage of non-masked pixels is called the acceptance. The hit efficiency was measured at the DESY-II testbeam facility [16] using a EUDET-type pixel beam telescope [17] for particle tracking. The data for the studies presented in this paper were taken with a 5.2 GeV/c electron beam. The hit efficiency times acceptance, the percentage of pixels masked as noisy, and the average noise occupancy are shown in Fig. 3 for two modules irradiated at the CERN PS. The fluence was distributed inhomogeneously over the modules and each module was sub-devided into several regions of equal fluence. Only pixels with a charge above a settable threshold are read out (about 1200 e^- if not mentioned otherwise). The time-over-threshold (ToT) is used as a measure of the charge recorded by a pixel. More details of this analysis can be found in Ref. [18].

The hit efficiency as a function of the threshold is shown in Fig. 4 for five fluence regions on two modules irradiated at the CERN PS for a bias voltage of 400 V and 600 V, respectively. For thresholds between 1500 and 2000 electrons, the hit efficiency drops below 98% at 600 V. The efficiency drop with threshold is much more pronounced at 400 V where low electric field regions reduce the charge collection. In order to achieve the target hit efficiency for fluences between $\Phi_{eq} = (0.5 - 1.0) \times 10^{16}$ cm^{-2}, it is hence required to be able to bias planar sensors to up to 600 V and to run at charge thresholds below around 1500 e.

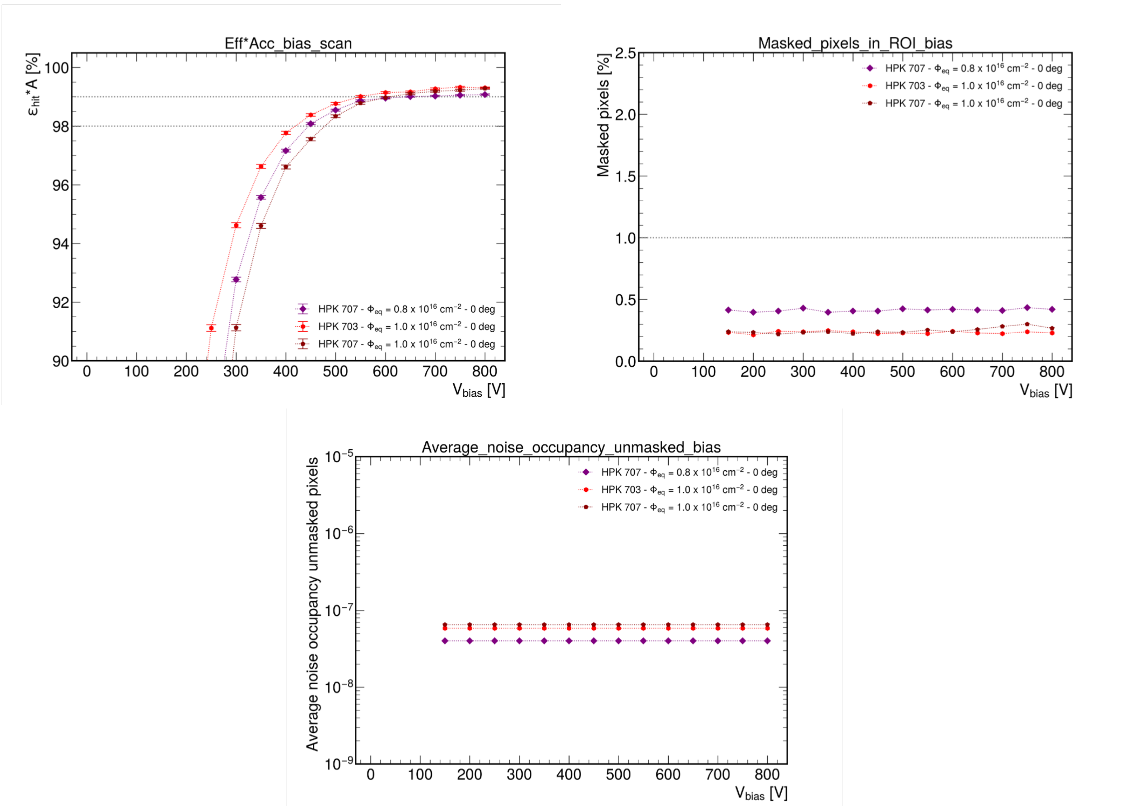

Figure 3: Hit efficiency*Acceptance (upper left), percentage of masked pixels (upper right), and noise occupancy (lower) for three fluence regions on two different CMS planar pixel sensor assemblies tuned to a threshold of about 1200 e$^-$. The requirements for the hit efficiency and the percentage of noisy pixels are indicated with horizontal lines.

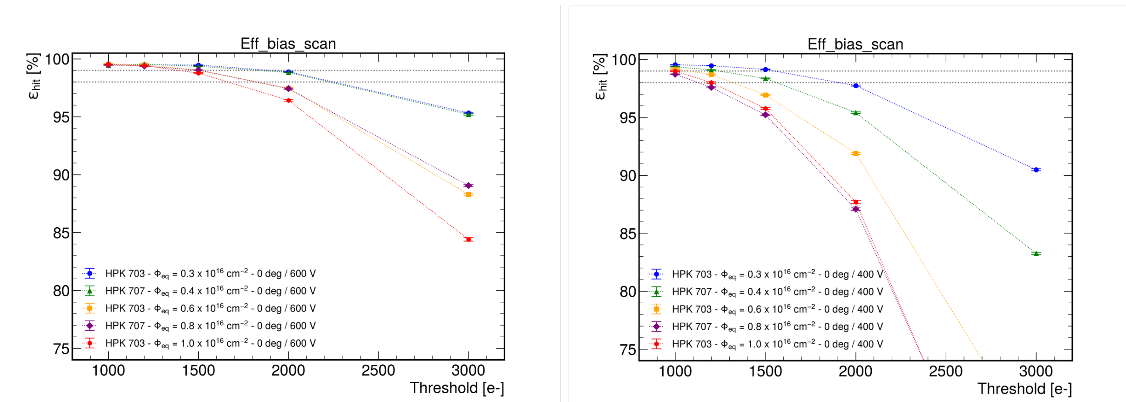

Figure 4: Hit efficiency as a function of threshold for a bias voltage of 600 V (left) and 400 V (right) for five fluence regions on two different CMS planar pixel sensor assemblies.

3. Spatial resolution

The spatial resolution as a function of the angle of incidence for rotations around the long pixel axis is shown in Fig. 5, before and after irradiation. The resolution is determined from the RMS of the residual distributions of the module cluster positions with respect to the telescope tracks, truncated at 3σ to reduce the impact of outliers. The telescope track resolution is then subtracted in quadrature, approximately 5 µm for the setup with the non-irradiated module, and 12 µm for the setup with the irradiated modules which required a cold box. The spatial resolution degrades with increasing fluence owing to a reduction in the signal-to-noise ratio and threshold effects. However, the resolution in both pixel directions stays well below the binary resolution expected for single hit clusters, marked as gray dashed lines, for all fluences.

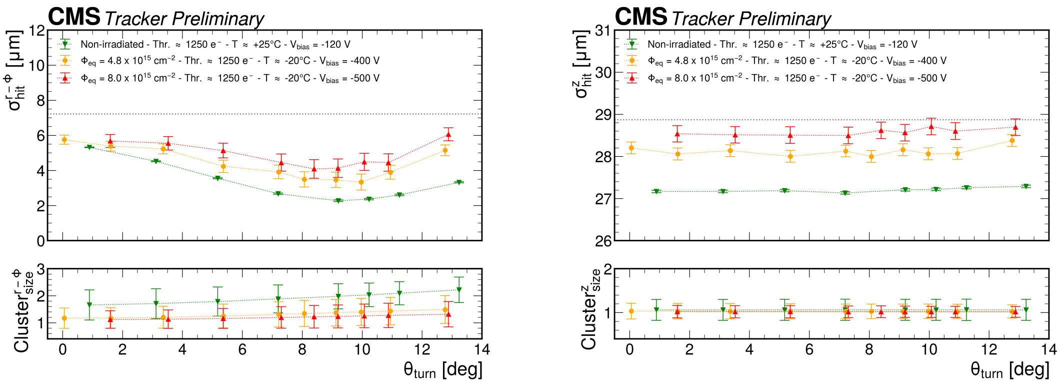

Figure 5: Spatial resolution and mean projected cluster size as a function of the turn angle for CROCv1 single chip planar pixel sensor assemblies before and after irradiation in the 25 µm (left) and 100 µm (right) direction.

4. 3D sensors

In the first layer of TBPX, 3D sensor modules composed of two individual sensors each interconnected to one CROCv2 readout chip will be used. The simulated thermal performance of planar and 3D modules is shown in Fig. 6. The plots show the difference between the CO_2 temperature and the temperature of the sensor as function of the CO_2 temperature. Above a certain CO_2 temperature, the cooling power for heavily irradiated sensors is insufficient and the temperature difference starts rising very quickly, a phenomenon known as thermal runaway. If the onset of thermal runaway is well above the nominal set point of the CO_2 temperature (−33 °C), there is enough margin to operate the module safely. The left plot is for a 3D sensor module in layer 1 of TBPX for a fluence of $\Phi_{eq} = 1.5 \times 10^{16}\,\text{cm}^{-2}$, whereas the right plot is for a planar sensor module in layer 2 of TBPX for a fluence of $\Phi_{eq} = 1 \times 10^{16}\,\text{cm}^{-2}$. It can be seen that 3D modules have a sufficient margin for thermal runaway in layer 1 of TBPX, whereas in layer 2 planar sensor modules are a safe choice. The hit efficiency and the percentage of pixels marked as noisy have been measured at the DESY-II testbeam for several 3D sensor assemblies with the CROCv1 chip irradiated with 23 GeV protons at the CERN PS to about $\Phi_{eq} = 1 \times 10^{16}\,\text{cm}^{-2}$. The modules reach the required efficiency of 96% at vertical track incidence at around 90 V, and the percentage of noisy pixels stays below about 1.5% below 150 V. The hit efficiency at close to vertical track incidence for 3D modules tends to be slightly lower than that for planar sensor modules owing to the columnar structure of the highly doped implants, which do not collect charge when the track hits them directly head on. The hit efficiency as a function of the position within a pixel cell for a bias voltage of 80 V (left) and 150 V (right) for an irradiated 3D single chip assembly is shown in Fig. 7. One can see inefficiencies in the corners of the pixel cell where the columns are, especially at the lower voltage. However, in the CMS IT, most tracks have a non-zero inclination angle with respect to the sensor normal and thus will never be fully contained in dead regions.

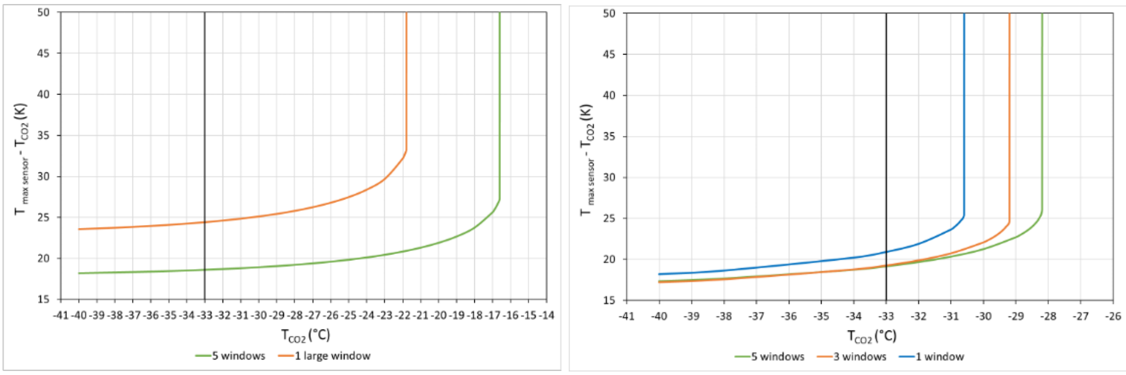

Figure 6: Simulated difference of the sensor and CO_2 temperature for a 3D sensor module in layer 1 of TBPX for a fluence of $\Phi_{eq} = 1.5 \times 10^{16}\,\mathrm{cm}^{-2}$ (left) and a planar sensor module in layer 2 of TBPX for a fluence of $\Phi_{eq} = 1 \times 10^{16}\,\mathrm{cm}^{-2}$ (right). Results for several designs of the cooling contact plate are shown with 1, 3, and 5 windows. While the 5 window design has the most material and hence the best thermal performance, the final choice is still open at the time of this writing.

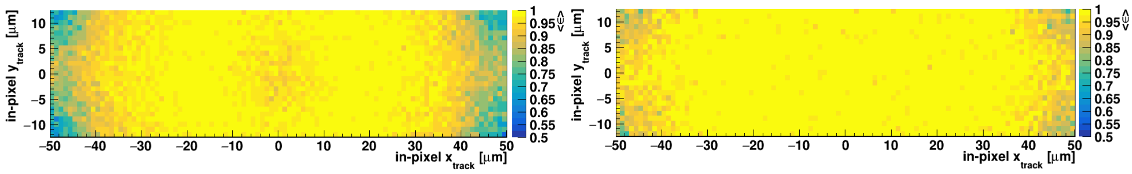

Figure 7: Hit efficiency as a function of the position within a pixel cell for a bias voltage of 80 V (left) and 150 V (right) for a 3D single chip assembly irradiated with 23 GeV protons at the CERN PS to about $\Phi_{eq} = 1 \times 10^{16}\,\mathrm{cm}^{-2}$.

5. Summary

The entire CMS tracking detector will be replaced for the High Luminosity running phase of the LHC. The Inner Tracker (IT) will feature planar sensors with a pixel size of $100\,\mu\mathrm{m} \times 25\,\mu\mathrm{m}$ everywhere except in the innermost layer of the barrel sections, where 3D sensors will be used because of their better radiation hardness and lower power consumption. As part of a qualification campaign, planar and 3D sensor assemblies with the full size prototype of the CMS readout chip, CROCv1, were tested in the DESY-II testbeam facility before and after irradiation at the CERN PS to fluences corresponding to the end-of-lifetime (or mid-run replacement for some assemblies). The hit efficiency, the percentage of noisy pixels, and the spatial resolution were measured under various operating conditions. The assemblies fulfill the requirements for the CMS IT. More generally, planar sensor modules will be useable up to fluences of about $\Phi_{eq} = 1 \times 10^{16}\,\mathrm{cm}^{-2}$, with thermal

runaway being the ultimate limiting factor and not the readout chip or sensor technology. The 3D sensor modules have been qualified to about $\Phi_{eq} = 1.5 \times 10^{16}\,\mathrm{cm}^{-2}$, above which an increase of the percentage of noisy pixels have been observed at the bias voltages needed for sufficient hit efficiency. Pixel module production for the final detector is planned to start in the second half of 2024.

6. Acknowledgments

This work was supported by the German Federal Ministry of Education and Research (BMBF) in the framework of the "FIS-Projekt - Fortführung des CMS-Experiments zum Einsatz am HL-LHC: Verbesserung des Spurdetektors für das Phase-2 Upgrade des CMS-Experiments". The measurements leading to these results have been performed at the Test Beam Facility at DESY Hamburg (Germany), a member of the Helmholtz Association (HGF). We also thank the team at the PS-IRRAD Proton Facility at CERN for their support.

References

[1] G. Apollinari et al., High-Luminosity Large Hadron Collider (HL-LHC): Technical Design Report V. 0.1, Technical Report CERN-2017-007-M, CERN, Geneva, 2017. URL: https://cds.cern.ch/record/2284929. doi:10.23731/CYRM-2017-004.

[2] High Luminosity LHC Project, 2023. URL: https://hilumilhc.web.cern.ch/.

[3] CMS Collaboration, The CMS Experiment at the CERN LHC, JINST 3 (2008) S08004. doi:10.1088/1748-0221/3/08/S08004.

[4] The Tracker Group of the CMS Collaboration, The CMS Phase-1 pixel detector upgrade, JINST 16 (2021) P02027. doi:10.1088/1748-0221/16/02/p02027.

[5] CMS Collaboration, The Phase-2 Upgrade of the CMS Tracker, Technical Report CERN-LHCC-2017-009, CERN, 2017. doi:10.17181/CERN.QZ28.FLHW.

[6] J. Duarte-Campderros et al., Results on proton-irradiated 3D pixel sensors interconnected to RD53A readout ASIC, Nucl. Instrum. Meth. A 944 (2019) 162625. doi:10.1016/j.nima.2019.162625.

[7] J. C. Christiansen M. L. Garcia-Sciveres (RD53 Collaboration), RD Collaboration Proposal: Development of pixel readout integrated circuits for extreme rate and radiation, Technical Report, CERN, Geneva, 2013. URL: https://cds.cern.ch/record/1553467.

[8] RD53B users guide, Technical Report, CERN, Geneva, 2020. URL: https://cds.cern.ch/record/2754251.

[9] M. Garcia-Sciveres, F. Loddo, J. Christiansen (RD53 Collaboration), RD53B Manual, Technical Report, CERN, Geneva, 2019. URL: https://cds.cern.ch/record/2665301.

[10] Hamamatsu Photonics K.K., 2021. URL: https://www.hamamatsu.com.

[11] Fondazione Bruno Kessler, 2017. URL: https://www.fbk.eu.

[12] J. Schwandt, CMS Pixel detector development for the HL-LHC, Nucl. Instrum. Meth. A 924 (2019) 59–63. doi:10.1016/j.nima.2018.08.121.

[13] The Tracker Group of the CMS Collaboration, Evaluation of HPK n^{+}-p planar pixel sensors for the CMS Phase-2 upgrade, Nucl. Instrum. Meth. A (2023) 168326. doi:10.1016/j.nima.2023.168326.

[14] The Tracker Group of the CMS Collaboration, Evaluation of planar silicon pixel sensors with the RD53A readout chip for the Phase-2 Upgrade of the CMS Inner Tracker, JINST 18 (2023) P11015. doi:10.1088/1748-0221/18/11/P11015.

[15] Fraunhofer Institute for Reliability and Microintegration IZM, 2021. URL: https://www.izm.fraunhofer.de/.

[16] R. Diener et al., The DESY II test beam facility, Nucl. Instrum. Meth. A 922 (2019) 265–286. doi:10.1016/j.nima.2018.11.133.

[17] H. Jansen et al., Performance of the EUDET-type beam telescopes, EPJ Tech. Instrum. 3, 7 (2016). doi:10.1140/epjti/s40485-016-0033-2.

[18] M. Antonello on behalf of the Tracker Group of the CMS Collaboration, Test beam results of irradiated modules for the CMS Phase-2 upgrade equipped with HPK planar pixel sensors and RD53B-CMS readout chips, Nucl. Instrum. Meth. A 1064 (2024). doi:10.1016/j.nima.2024.169379.